

New Physics contamination to precision luminosity measurements at future e^+e^- colliders

Mauro Chiesa,^{*} Oreste Nicosini,[†] and Fulvio Piccinini[‡]
INFN, Sezione di Pavia, Via A. Bassi 6, 27100 Pavia, Italy

Clara L. Del Pio[§]
Department of Physics, Brookhaven National Laboratory, Upton, NY 11973, U.S.A.

Guido Montagna[¶] and Francesco P. Ucci^{**}
*Dipartimento di Fisica, Università di Pavia, Via A. Bassi 6, 27100 Pavia, Italy and
INFN, Sezione di Pavia, Via A. Bassi 6, 27100 Pavia, Italy*

Several key observables of the high-precision physics program at future lepton colliders will critically depend on the knowledge of the absolute machine luminosity. The determination of the luminosity relies on the precise knowledge of some reference process, which is in principle not affected by unknown physics, so that its cross section can be computed within a well-established theory, like the Standard Model. Quantifying the uncertainties induced by possible New Physics effects on such processes is therefore crucial. We present an exploratory investigation of light and heavy New Physics contributions to the small-angle Bhabha process at future e^+e^- colliders and we discuss possible strategies to remove potential uncertainties originating from such contaminations by relying on observables that are independent of the absolute luminosity.

I. INTRODUCTION

The absolute luminosity measurement is extremely important at e^+e^- colliders, from low to high energy, because it is a source of systematics in the measurement of the cross section of several signal processes. For instance, at the few-GeV scale of flavour factories, it is crucial for the determination of the pion form factor through the measurement of the hadronic cross section in e^+e^- collisions [1], while at the energies of Z factories, like LEP in the past and CEPC/FCCee in the future, it is relevant for the determination of some key Standard Model (SM) parameters [2]. An example of the importance of a precise knowledge of the absolute luminosity is given by the recent study of the effects of beam-beam interactions at LEP [3], where an underestimate of the LEP luminosity of about 0.1% was discovered, removing a long-standing tension on the number of light neutrino species from LEP [4].

At future e^+e^- Higgs/Top/ElectroWeak factories, the luminosity calibration will also play a crucial role for the determination of the W boson mass and width at the WW threshold, as well as the effective HZZ coupling and the total Higgs boson width through the measurement of the total cross section of the process $e^+e^- \rightarrow HZ$ at energy scales of the order of 250 GeV [5].

The time-integrated luminosity L is related to the cross

section σ_0 of some reference process through the relation

$$L = \int \mathcal{L} dt = \frac{N_0}{\epsilon \sigma_0}, \quad (1)$$

where \mathcal{L} is the instantaneous luminosity, N_0 is the number of observed events of such a process and ϵ is the experimental selection efficiency. On the one hand, the choice of the reference processes is motivated by clean experimental signatures and large cross sections, in order to minimise the experimental systematics. On the other hand, a further important requirement is the feasibility of a very precise theoretical description of the differential cross sections of the reference process, as the precision in the cross section calculation enters directly as a source of systematics. At LEP, the above conditions were satisfied by small angle Bhabha scattering (SABS), where the process was largely dominated by t -channel photon exchange and the approximate modeling of the weak-interaction contributions was not a matter of concern. At flavour factories, the main reference process is large-angle Bhabha scattering (LABS) [1] and the processes $e^+e^- \rightarrow \mu^+\mu^-$ and $e^+e^- \rightarrow \gamma\gamma$ are also used for normalization and cross checks.

The highest relative experimental precision in the absolute luminosity calibration was achieved by the OPAL Collaboration [6] at LEP, with the value of 3.4×10^{-4} . At future high energy e^+e^- colliders, the precision requirements for the luminosity measurements will be even more demanding, being of the order of at least 10^{-4} , or possibly better, at the Z resonance and at the WW threshold region, and of the order of 10^{-3} at center of mass (c.m.) energies larger than about 240 GeV [5]. On the theoretical side, studies on the needs for the SM calculations and Monte Carlo event generators to reach such unprecedented precisions have appeared recently in the literature [7–13].

^{*} mauro.chiesa@pv.infn.it

[†] oreste.nicosini@pv.infn.it

[‡] fulvio.piccinini@pv.infn.it

[§] cdelpio@bnl.gov

[¶] guido.montagna@unipv.it

^{**} francesco.ucci@pv.infn.it

In this Letter, we investigate whether some contamination from New Physics (NP) could be present in the absolute luminosity measurement at various options for future high-energy e^+e^- colliders through SABS, by using the present and projected knowledge of the bounds on Beyond the Standard Model (BSM) effects. A preliminary investigation in this direction was presented in [14] for the process $e^+e^- \rightarrow \gamma\gamma$, which is presently under consideration as an alternative luminosity process [5, 15, 16]. Additionally, we explore the effectiveness of the asymmetry measurements of LABS as a tool to remove the uncertainties due to possible NP contributions.

II. NEW PHYSICS IMPACT ON SABS

The NP contributions can be due to heavy new degrees of freedom (d.o.f.) or to light mediators with feeble couplings to the leptons or photons which have escaped detection until now. For the former case, the natural framework for a model-independent analysis is the Standard Model Effective Field Theory (SMEFT), where all possible dimension-six operators are added to the SM Lagrangian. For the latter case of light NP contributions, a model dependent analysis is necessary. We will therefore study the effects due to the exchange of light d.o.f. with spin 0 or 1.

We consider in this analysis various future e^+e^- collider options, in particular FCC [17, 18]/CEPC [19, 20], ILC [21–25] and CLIC [26–28]. The angular acceptances of the luminometers and c.m. energies of the colliders are specified in the second and third columns of Tab. I, respectively. For the electroweak (EW) sector, we adopt the $\{\alpha(M_Z), G_\mu, M_Z\}$ input parameter scheme with $\alpha(M_Z) = 1/127.95$, $G_\mu = 1.16638 \times 10^{-5} \text{ GeV}^{-2}$ and $M_Z = 91.1876 \text{ GeV}$. The relevant amplitudes have been generated with FEYNARTS [29] and FEYNALC [30, 31]. For the SMEFT, we have used the UFO model from SMEFTFR [32–34] and checked against SMEFTSIM [35, 36] within MG5_AMC@NLO [37], while for light NP the used Lagrangians have been implemented in FEYNRULES [38]. The simulations have been performed with an updated version of the BABAYAGA@NLO Monte Carlo generator [39–43], for both light and heavy NP contributions.

A. Light New Physics scenarios

If the mass of NP is below the EW scale, i.e. $M_{\text{NP}} \lesssim \Lambda_{\text{EW}}$, an EFT approach is not suitable and we need to rely on specific models. Inspired by [44], we analyse the maximal contamination of coupling to (pseudo)scalar, (axial)vector NP d.o.f. that are not excluded by the current experimental bounds. As shown in the following, the numerical results obtained with BABAYAGA@NLO can be understood by considering the analytical estimate of

the leading light NP deviations given by

$$\delta_{\text{LNP}} \simeq \frac{2 \text{Re}(\mathcal{M}_\gamma(t)^\dagger \mathcal{M}_{\text{LNP}})}{|\mathcal{M}_\gamma(t)|^2}, \quad (2)$$

where the subscript γ indicates the photon exchange, which dominates the SM SABS cross section.

1. (Pseudo)scalar ALPs

The interaction of a (pseudo)scalar axion-like particle (ALP) a of mass m_a with both the photon and the electron can be parameterised with the parity-violating Lagrangian

$$\begin{aligned} \mathcal{L}_{\text{ALP}} = & \frac{1}{2} \partial_\mu a \partial^\mu a - \frac{1}{2} m_a^2 a^2 \\ & + \frac{1}{4} g_{a\gamma\gamma} (F_{\mu\nu} \tilde{F}^{\mu\nu}) a + g_{aee} (\bar{e} i\gamma_5 e) a, \end{aligned} \quad (3)$$

where $F_{\mu\nu}$ is the electromagnetic field tensor, $\tilde{F}^{\mu\nu}$ the dual field tensor and e the electron field. In Eq. 3, the scalar parity-conserving case is obtained with the substitutions $\tilde{F}^{\mu\nu} \rightarrow F^{\mu\nu}$, $i\gamma_5 \rightarrow \mathbb{I}$. In the limit $m_a \ll \sqrt{s}$, the leading contribution in g_{aee} is given by the interference of the t -channel photon exchange with the s -channel diagram mediated by the ALP, as $\mathcal{M}_\gamma^\dagger(t) \mathcal{M}_a(t)$ vanishes in the limit $m_e \simeq 0$, yielding to a relative differential deviation given by

$$\delta_{\text{ALP}}^{\text{aee}} \simeq \frac{g_{aee}^2}{4\pi\alpha} \frac{s^2 t}{(s - m_a^2)(s^2 + u^2)} \simeq -\frac{g_{aee}^2}{8\pi\alpha} (1 - \cos\theta), \quad (4)$$

which is highly suppressed at small angle. In order to evaluate the maximal effect, we consider the largest unconstrained coupling, given by $(g_{aee}, m_a) \simeq (3 \times 10^{-3}, 1 \text{ GeV})$ [45], yielding $\delta_{\text{ALP}}^{\text{aee}} < 10^{-7}$ for small angles, well below any future collider precision goal. A light ALP can be also produced via photon fusion in the process $e^+e^- \rightarrow \gamma^* \gamma^* e^+e^- \rightarrow e^+e^- a$, that can give the same experimental signature of SABS [46]. For this process, the results have been obtained with a modified version of the code for $\pi^0 \pi^0$ [47] and η [48] production in e^+e^- collisions and π^0 production in μe scattering [49]. For $g_{a\gamma\gamma} = 2 \times 10^{-4} \text{ GeV}^{-1}$ [50], this contribution at the Z peak in a small angular acceptance is suppressed, giving $\delta_{\text{ALP}}^{\text{a}\gamma\gamma} \sim \mathcal{O}(10^{-6})$. At higher energy, the bulk of the axion emission cross section is unchanged, while the SM cross section falls as $1/s$, yielding to $\delta_{\text{ALP}}^{\text{a}\gamma\gamma}(1 \text{ TeV}) \sim \mathcal{O}(10^{-5})$. This feature can be understood since the total cross section for axion emission grows logarithmically with the c.m. energy [51] but the angular distribution of the electron and positron around the beam axis becomes more sharply peaked. The fixed angular acceptance effectively removes the cross section at high energies.

2. Dark Vectors

In a light NP scenario, Bhabha scattering could also be mediated by a dark vector boson V_μ associated with a new gauge group $U(1)'$. The kinetic mixing of this boson [52–54] with the SM (un)broken $U(1)_{\text{(em)Y}}$ gauge field would result in a coupling with the electromagnetic current after EW symmetry breaking. In the literature, such scenarios, that could explain the relic abundance of Dark Matter in the Universe, are usually referred to as Dark photons [55] or light Z' models [56]. The Lagrangian we use to estimate such effects is given by

$$\begin{aligned} \mathcal{L}_{\text{Dark}} = & -\frac{1}{4}V^{\mu\nu}V_{\mu\nu} + \frac{1}{2}M_V^2 V_\mu V^\mu \\ & + g'_V (\bar{e} \gamma^\mu e) V_\mu + g'_A (\bar{e} \gamma^\mu \gamma_5 e) V_\mu, \end{aligned} \quad (5)$$

where $g'_{V,A}$ are the vector/axial couplings of the dark spin-1 mediator of mass M_V with electrons and $V_{\mu\nu}$ is the dark field tensor. The bulk of the deviation w.r.t. the SABS in the SM due to dark vectors is given by the interference of the QED with the dark vector t -channel exchange, i.e.

$$\delta_{\text{Dark}} \simeq \frac{t \left[g_V'^2 (s^2 + u^2) - g_A'^2 (s^2 - u^2) \right]}{2\pi\alpha (t - M_V^2) (s^2 + u^2)}. \quad (6)$$

At small angles, one has $u \simeq -s$, resulting in a strongly suppressed axial coupling. The maximal contribution of the vector dark current is given for $(g'_V, M_V) \simeq (3 \times 10^{-4}, 1 \text{ GeV})$ [45, 50], resulting in $\delta_{\text{Dark}} \sim \mathcal{O}(10^{-6})$, which is more than two orders of magnitude below the foreseen luminosity precision of future colliders.

B. Heavy New Physics scenarios

Under the assumption that the NP scale lies far above the electroweak scale, i.e. $\Lambda_{\text{NP}} \gtrsim \mathcal{O}(\text{TeV})$, one can study deviations from the SM using the SMEFT framework at dimension six (see Ref. [57] for a review), a model-independent way to capture the leading BSM effects. The effective Lagrangian is expanded about the SM as follows

$$\mathcal{L}_{\text{SMEFT}} = \mathcal{L}_{\text{SM}} + \sum_i \frac{C_i \hat{O}_i^{(6)}}{\Lambda_{\text{NP}}^2} + \mathcal{O}\left(\frac{1}{\Lambda_{\text{NP}}^4}\right), \quad (7)$$

where the operators $\hat{O}_i^{(6)}$ are built from the same d.o.f. of the SM as gauge invariant combinations under $SU(3)_C \times SU(2)_L \times U(1)_Y$ and C_i are the associated Wilson Coefficients (WCs). In the following, we do not make any flavour symmetry assumption, therefore considering a completely general flavour scenario. The EW Lagrangian

in the $\{\alpha, G_\mu, M_Z\}$ scheme reads [58]

$$\begin{aligned} \mathcal{L}_{\text{SMEFT}}^{\text{EW}} = & -\sqrt{4\pi\alpha} (\bar{e} \gamma^\mu e) A_\mu \\ & + \frac{\sqrt{4\pi\alpha}}{s_w c_w} \left[\bar{e}_L \gamma^\mu \left(\hat{g}_L + \frac{\Delta g_L^{Ze}}{\Lambda_{\text{NP}}^2} \right) e_L \right. \\ & \left. + \bar{e}_R \gamma^\mu \left(\hat{g}_R + \frac{\Delta g_R^{Ze}}{\Lambda_{\text{NP}}^2} \right) e_R \right] Z_\mu, \end{aligned} \quad (8)$$

where A_μ and Z_μ are the photon and Z -boson field, respectively and $e_{L,R}$ are the left and right-handed electron fields. In Eq. 8, the sine of the weak mixing angle is defined as $s_w^2 = \frac{1}{2} \left(1 - \sqrt{1 - 2\sqrt{2}\pi\alpha/G_\mu M_Z^2} \right)$ and the effective shifts $\Delta g_{L(R)}^{Ze}$ parameterise the SMEFT deviations from the SM left- and right-handed couplings of the Z boson to electrons, namely $\hat{g}_L = s_w^2 - 1/2$ and $\hat{g}_R = s_w^2$. Their expressions in the Warsaw basis [59], given in Appendix A, are linear combinations of WCs acting as effective eeV couplings due to new interactions or modifications of the electroweak symmetry breaking and enter the muon decay width when choosing G_μ as input. We stress that if the electromagnetic coupling is not taken as an input also an overall $\Delta\alpha \neq 0$ shift is present at dimension six [36, 60]. In view of the bounds on $\Delta g_{L(R)}^{Ze}$ [58], their contribution to the SABS cross section is negligible.

At dimension six, also four-fermion contact interactions contribute to the Bhabha cross section. Their Lagrangian is independent of the input scheme and reads as follows

$$\begin{aligned} \mathcal{L}_{\text{SMEFT}}^{4f} = & \frac{1}{2} \frac{C_{ll}}{\Lambda_{\text{NP}}^2} (\bar{e}_L \gamma^\mu e_L) (\bar{e}_L \gamma_\mu e_L) \\ & + \frac{C_{le}}{\Lambda_{\text{NP}}^2} (\bar{e}_L \gamma^\mu e_L) (\bar{e}_R \gamma_\mu e_R) \\ & + \frac{1}{2} \frac{C_{ee}}{\Lambda_{\text{NP}}^2} (\bar{e}_R \gamma^\mu e_R) (\bar{e}_R \gamma_\mu e_R), \end{aligned} \quad (9)$$

where the $1/2$ factors take into account the exchange of two identical currents.

In order to quantify the leading deviation from the SM, we systematically neglect $\mathcal{O}(\Lambda_{\text{NP}}^{-4})$ terms when computing predictions and work at leading order (LO) in the SMEFT couplings. Systematic analyses at next-to-leading order (NLO) in the SMEFT have been carried out for specific observables [61–65], while global analysis have been performed at (partial) NLO accuracy in the SMEFT and including the effects of Renormalization Group Evolution [66, 67]. Limiting the discussion to the four-fermion operators, which give the leading contribution to the uncertainties from NP to SABS, the NLO correction to operators already appearing at LO is roughly of $\mathcal{O}\left(\frac{\alpha}{\pi} \ln \frac{\Lambda_{\text{NP}}^2}{|t|}\right)$. With t the typical scale of the reference process and $\Lambda_{\text{NP}} \sim 1 \text{ TeV}$, we conservatively get a contribution of the order of 10% relative to the LO SMEFT prediction. Concerning \hat{O}_j operators not appearing at

Exp.	$[\theta_{\min}, \theta_{\max}]$	\sqrt{s} [GeV]	$(\delta \pm \Delta\delta)_{\text{SMEFT}}$	$\Delta L/L$
FCC	[3.7°, 4.9°]	91	$(-4.2 \pm 1.7) \times 10^{-5}$	$< 10^{-4}$
		160	$(-1.3 \pm 0.5) \times 10^{-4}$	
		240	$(-2.9 \pm 1.2) \times 10^{-4}$	10^{-4}
		365	$(-6.7 \pm 2.7) \times 10^{-4}$	
ILC	[1.7°, 4.4°]	250	$(-2.5 \pm 0.9) \times 10^{-4}$	$< 10^{-3}$
		500	$(-4.9 \pm 1.9) \times 10^{-4}$	
CLIC	[2.2°, 7.7°]	1500	$(-9.7 \pm 3.9) \times 10^{-3}$	
		3000	$(-4.2 \pm 1.7) \times 10^{-2}$	$< 10^{-2}$

TABLE I. Heavy NP contamination to SABS as in Eq. 11 at future e^+e^- facilities. $\Delta L/L$ represents the luminosity target precision.

tree level, they contribute to the SABS cross section as $\frac{|t|}{\Lambda_{\text{NP}}^2} \frac{C_j}{16\pi^2} \log \frac{\Lambda_{\text{NP}}^2}{|t|} \sim 10^{-3} C_j$, which is not expected to alter significantly the LO results.

At LO SMEFT, the prediction for the Bhabha cross section is given by

$$\sigma_{\text{SMEFT}} = \sigma_{\text{SM}} + \sigma^{(6)} = \sigma_{\text{SM}} + \sum_{i=1}^n \frac{C_i}{\Lambda_{\text{NP}}^2} \sigma_i^{(6)}, \quad (10)$$

where $\sigma_i^{(6)} = 2 \text{Re} \mathcal{M}_{\text{SM}}^\dagger \mathcal{M}_{\text{SMEFT},i}^{(6)}$ is the interference between the SM and SMEFT amplitude due to the i -th coefficient, having factored out the dependency on the ratio of the WCs to the NP scale. We set $\Lambda_{\text{NP}} = 1 \text{ TeV}$, the EFT validity being ensured, as at small angle the relevant scale of the process is $t = -s/2(1 - \cos \theta_{\min})$, which is at most $\mathcal{O}(50 \text{ GeV})$ for $s = 3 \text{ TeV}$ in the CLIC setup. We define the deviation from SM (differential) cross sections due to heavy NP

$$(\delta \pm \Delta\delta)_{\text{SMEFT}} = \frac{1}{\sigma_{\text{SM}}} \left(\sigma^{(6)} \pm \sqrt{\sum_{ij} \sigma_i^{(6)} V_{ij} \sigma_j^{(6)}} \right), \quad (11)$$

where the covariance matrix $V_{ij} = \Delta(C_i) \rho_{ij} \Delta(C_j)$ takes into account the correlation between fitted coefficients and their errors. We use the flavour-general bounds on coefficients and correlation matrix from the global fit of Ref. [58], that include EW and low-energy precision data, as quoted in Appendix A.

In Table I we show the uncertainty for SABS due to heavy NP deviation for SABS in the luminometer setup of future colliders. It can be seen that possible BSM effects would affect the luminosity precision target of future e^+e^- facilities in a non-negligible way [68]. With polarised beams at ILC and CLIC, the results can worsen up to a factor of two. We have also checked that NP uncertainties are below the precision goal of the luminosity determination at LEP with SABS and at BELLE-II with LABS.

The foreseen HL-LHC data are not expected to further constrain significantly the four-electron WCs, as dis-

cussed for example in [67], in which the estimated reduction is of $\sim 20\%$ only. As discussed in the following, a possible strategy is to constrain the contact operators directly at future e^+e^- accelerators, by using observables that are independent of the absolute luminosity and can be measured with high precision.

III. CONSTRAINING CONTACT INTERACTIONS WITH LABS

In the worst-case scenario of no significant improvement on WCs bounds by the timeline of the start of future colliders, we explore in this Section the possibility of constraining such coefficients using observables that do not depend on the luminosity. Suitable quantities to this purpose are asymmetries, as they depend only on the number of events counted in the detector, as the luminosity cancels in the ratio. If asymmetries related to the LABS process can be exploited, no additional assumptions on the NP scenarios are needed. Assuming lepton flavor universality, asymmetries related to $\mu^+\mu^-$ and $\tau^+\tau^-$ pair production could also be used, providing more constraining power. Throughout this section we consider the LABS in the $\theta \in [40^\circ, 140^\circ]$ acceptance motivated by LEP analyses [69]. We assume the validity of the SM and focus on the attainable uncertainties of the WCs by future asymmetry data [70].

A. The Z resonance region

In the energy region close to the Z resonance, the lepton forward-backward asymmetry $A_{\text{FB}}^{\ell\ell}$ is expected to be particularly useful. We consider the tree-level SMEFT prediction for the LABS $A_{\text{FB}}(\sqrt{s})$ neglecting the shifts of the Z couplings and considering only the dependence on the $\vec{C}_{4f} = (C_{ll}, C_{le}, C_{ee})$ coefficients. The measurement of $A_{\text{FB}}(\sqrt{s})$ at three different values of \sqrt{s} can provide the necessary information to constrain the three WCs \vec{C}_{4f} . The three energy points more sensitive to deviations from the SM can be identified by calculating the difference between the prediction in the SM and in the SMEFT with current bounds on \vec{C}_{4f} , as shown in Fig. 1. They are found as the two local minima located at $\sqrt{s_1} = 89 \text{ GeV}$, $\sqrt{s_3} = 98 \text{ GeV}$ and the maximum at $\sqrt{s_2} = 93 \text{ GeV}$. It is worth stressing that the radiative corrections will play an important role, in particular in the choice of the optimal energy points [71].

Therefore, we write the relative deviation of $A_{\text{FB}}^e(\sqrt{s}_\alpha)$ in the SMEFT as [72]

$$\sum_{i \in 4f} \frac{C_i}{\Lambda_{\text{NP}}^2} \left[\frac{(\sigma_{\text{F}} - \sigma_{\text{B}})_i^{(6)}}{(\sigma_{\text{F}} - \sigma_{\text{B}})_{\text{SM}}} - \frac{(\sigma_{\text{F}} + \sigma_{\text{B}})_i^{(6)}}{(\sigma_{\text{F}} + \sigma_{\text{B}})_{\text{SM}}} \right]_\alpha = \frac{\Delta A_{\text{FB},\alpha}^0}{A_{\text{FB},\alpha}^0}, \quad (12)$$

where $\alpha = \{1, 2, 3\}$ labels the energy point and $\sigma_{\text{F}} = \int_0^{c_{\text{max}}} dc \left(\frac{d\sigma}{dc} \right)$ and $\sigma_{\text{B}} = \int_{-c_{\text{max}}}^0 dc \left(\frac{d\sigma}{dc} \right)$ are the for-

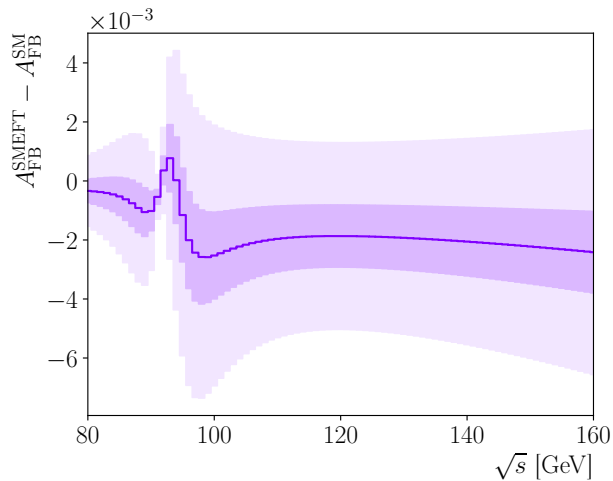


FIG. 1. Absolute deviation of the LABS A_{FB} predicted in the SMEFT and the SM, using the current knowledge on WCs. The solid line is the central value whereas the shaded regions are the 1σ and 3σ uncertainty bands.

ward/backward cross sections, in which $c = \cos\theta$ and $c_{\text{max}} = 0.77$ is a realistic cut for the LABS. In order to have a quantitative estimate of the uncertainty reduction for four-electrons WCs at FCCee/CEPC, we solve the system by generating MC replicas of the experimental value $A_{\text{FB}}^0 \sim g(A_{\text{FB}}^{\text{SM}}, \Delta A_{\text{FB}}^0)$ as a Gaussian centered about the SM tree-level prediction with statistical error $\Delta A_{\text{FB}}^{0,ee}$. Considering one year of run (10^7s) for each \sqrt{s}_α with an FCC-like instantaneous luminosity $\mathcal{L}_{\text{FCC}} = 1.4 \times 10^{36} \text{ cm}^{-2} \text{ s}^{-1}$ [17], we find $\Delta A_{\text{FB},\alpha}^0 \lesssim 2 \times 10^{-5}$. The 1σ uncertainty on four-electrons coefficients is reduced to $\Delta C_{ll/ee} \lesssim 10^{-2}$ and $\Delta C_{le} \lesssim 10^{-3}$ yielding to $\delta_{\text{SMEFT}} \sim 5 \times 10^{-6}$ on the Z -peak luminosity at FCC, below the precision goal. This constraint would be enough also for future e^+e^- colliders runs at higher energies.

B. The high energy region

In the scenario of high-energy future machines that will not revisit the Z resonance scan, the A_{FB} observable can not be used to constrain the four-fermion WCs, as it is almost constant for $\sqrt{s} \gtrsim 120 \text{ GeV}$. Since linear collider projects feature polarised beams, we investigate the possibility of using polarization asymmetries for LABS at fixed \sqrt{s} and different angles assuming that they are independent of the luminosity [73]. We the ILC 250 GeV run [74], with the expected luminosity of $\mathcal{L}_{\text{ILC}} = 1.35 \times 10^{34} \text{ cm}^{-2} \text{ s}^{-1}$. For longitudinally polarised beams with fraction P_{e^\pm} of polarised positrons/electrons, the differential cross section in the scattering angle can be written as

$$\frac{d\sigma(P_{e^\pm})}{d\cos\theta} = \frac{1}{4} \sum_{I,J=L,R} (1 + P_{e_I^+})(1 + P_{e_J^-}) d\sigma_{e_I^+ e_J^-} \quad (13)$$

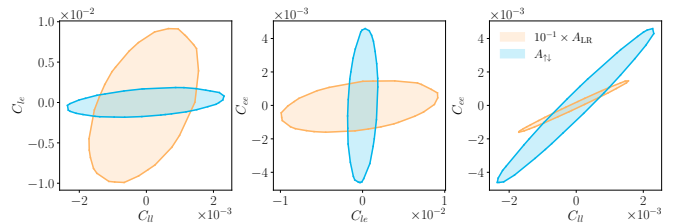


FIG. 2. Results of the χ^2 fit at 68% confidence level projected in 2-dimensional subspaces. As it can be seen in the third panel, the fit of A_{LR} manifests an approximate flat direction in the (C_{ll}, C_{ee}) plane.

where $P_{e_R^\pm} = P_{e^\pm}$ and $P_{e_L^\pm} = -P_{e^\pm}$, with the proposed values $|P_{e^-}| = 0.8$ and $|P_{e^+}| = 0.3$. The theoretical prediction for polarisation asymmetries $A_{\text{pol}}^{\text{th}}$ built from the SMEFT calculation of $d\sigma(P_{e^\pm})/d\cos\theta$, defined in Eq. 13, is dependent of the WCs. Therefore, such asymmetries can be exploited to fit the confidence intervals of \vec{C}_{4f} by means of a χ^2 fit over n independent bins

$$\chi^2 = \sum_{\alpha=1}^n \frac{\left(A_{\text{pol}}^0 - A_{\text{pol}}^{\text{th}}(\vec{C}_{4f})\right)_\alpha^2}{(\Delta A_{\text{pol}}^0)_\alpha^2}, \quad (14)$$

where the assumptions on the experimental value A_{pol}^0 and its error are the same as the previous section. Further details on the fit methodology are given in Appendix B.

The commonly measured left-right asymmetry is defined as $A_{\text{LR}}^{\text{ff}} = (\sigma_L - \sigma_R)/(\sigma_L + \sigma_R)$, where the right cross section σ_R is obtained by measuring the quantity of Eq. (13) for a fixed set (P_{e^+}, P_{e^-}) and the left one σ_L is obtained by inverting the sign of the polarizations. This observable was used at the SLD experiment at SLC for a precision measurement of $\sin^2\theta_{\text{eff}}^l$ [75, 76] and it can be effective in future precision tests of the SM and of NP scenarios [22, 77–79]. Unfortunately, as shown in the third panel of Figure 2, such asymmetry exhibits an almost exact flat direction as $C_{ll} \simeq C_{ee}$ due to its mild sensitivity to C_{le} , whose contribution depends on the product $P_{e^+}P_{e^-}$ and hence cancels in the numerator of A_{LR} . Therefore, in analogy with A_{LR} , we propose the following differential up-down asymmetry for a fixed \sqrt{s}

$$A_{\uparrow\downarrow}^-(P_{e^\pm}, \cos\theta) = \frac{d\sigma(P_{e^-}, P_{e^-}) - d\sigma(P_{e^+}, -P_{e^-})}{d\sigma(P_{e^+}, P_{e^-}) + d\sigma(P_{e^+}, -P_{e^-})}, \quad (15)$$

inverting the sign of P_{e^-} . In Figure 2 we show the results of the χ^2 fit for $A_{\text{pol}} = A_{\text{LR}}, A_{\uparrow\downarrow}^-$ projected into 2D subspaces at 68% confidence level. While A_{LR} does not constrain further \vec{C}_{4f} , using the up-down asymmetry the uncertainty ΔC_i is reduced to a few 10^{-3} for all four-electron WCs. This would correspond to a negligible effect of $\delta_{\text{SMEFT}} \lesssim 10^{-7}$ on the SABS luminosity measurements.

IV. CONCLUSIONS

Assessing the NP contamination to luminosity measurements will be crucial to achieve the precision physics program at future e^+e^- colliders. In this Letter, we have studied the BSM effects to the reference process SABS using an improved version of the BABAYAGA@NLO event generator, that simulates the Bhabha cross section including both light and heavy NP d.o.f.

We have shown that the impact of light new scalars and vectors on the absolute luminosity is well below the expected experimental uncertainties for all scenarios.

The heavy NP contributions have been parameterised in a model-independent way, within the SMEFT framework. We have shown that the shifts of the SM Zee couplings are irrelevant, whereas the uncertainties to the SABS due to four-electron operators are not negligible around the Z resonance, as well as at higher energies.

In order to overcome these uncertainties, we have proposed possible strategies which rely on observables at large angle that are independent of the absolute luminosity. The contamination due to heavy NP could be removed by a measurement of the forward-backward asymmetry A_{FB} of the LABS process at three different c.m. energy points close to the Z resonance. These measurements would be also enough for removing any possible bias at higher energies.

If a run around the Z resonance is not foreseen by future e^+e^- machines, the beam polarisation could allow to constrain the relevant WCs. In particular, we have proposed a new kind of polarization asymmetry that would provide more constraining power than the left-right asymmetry A_{LR} , reducing the four-electron contamination to the luminosity below the target precision.

The results of the present work could be put on firmer ground by including in our study the contribution of NLO corrections in the SM and SMEFT. This analysis is left to future work. We plan to further investigate the NP contamination to other relevant processes for precision luminosity monitoring at future lepton facilities, such as two photon production in e^+e^- annihilation and $\mu^+\mu^- \rightarrow \mu^+\mu^-$ at a muon collider.

V. ACKNOWLEDGMENTS

We are indebted to Carlo M. Carloni Calame and Mauro Moretti for useful discussions. We thank Ilaria Brivio and Luca Mantani for helpful advice on SMEFT global fits and Marco Zaro for assistance with MG5_AMC@NLO. The authors are grateful to Alain Blondel, Roberto Tenchini, Graham Wilson and Dirk Zerwas for fruitful feedback on the experimental side. We also acknowledge Juan Alcaraz Maestre for interest in our work. C.L.D.P. is supported by the US Department of Energy under Grant Contract DE-SC0012704.

Appendix A: Numerical values of Wilson Coefficients

In this Appendix we give further details on the WCs used in this work. We recall that the shifts to the Zee SM couplings are defined in terms of the Warsaw basis as [58]

$$\begin{aligned}\Delta g_L^{Ze} &= \frac{1}{\Lambda_{\text{NP}}^2} \left\{ -\frac{1}{2}[C_{HI}]_{11}^{(3)} - \frac{1}{2}[C_{HI}]_{11}^{(1)} + f\left(-\frac{1}{2}, -1\right) \right\} \\ \Delta g_R^{Ze} &= \frac{1}{\Lambda_{\text{NP}}^2} \left\{ -\frac{1}{2}[C_{HI}]_{11}^{(1)} + f(0, -1) \right\},\end{aligned}$$

with

$$\begin{aligned}f(T^3, Q) &= -Q \frac{s_w c_w}{c_w^2 - s_w^2} C_{HWB} \\ &+ \left(\frac{1}{4}[C_U]_{1221} - \frac{1}{2}[C_{HI}]_{11}^{(3)} - \frac{1}{2}[C_{HI}]_{22}^{(3)} - \frac{1}{4}C_{HD} \right) \times \\ &\left(T^3 + Q \frac{s_w^2}{c_w^2 - s_w^2} \right),\end{aligned}$$

where T_3 and Q are the third component of the isospin and the charge of the electron, respectively, and the pedices indicate the flavour index $\{1, 2, 3\} = \{e, \mu, \tau\}$. The translation to other basis can be found in [80].

In Table II we report the central values and the errors at 68% confidence level for the Zee couplings shifts and the four-electrons WCs used as input for the results of Table I and Figure 1. The values of C_i are given for $\Lambda_{\text{NP}} = 1 \text{ TeV}$. The corresponding correlation matrix is

C_i	$C_i \pm \Delta(C_i)$
Δg_L^{Ze}	-0.0038 ± 0.0046
Δg_R^{Ze}	-0.0054 ± 0.0045
C_U	0.17 ± 0.06
C_{le}	-0.037 ± 0.036
C_{ee}	0.034 ± 0.062

TABLE II. Central values and 68% uncertainty of the WCs, taken from the flavour general results of Eq. (4.8) of [58].

given by

$$\rho^{\text{General}} = \begin{pmatrix} 1 & & & & \\ 0.15 & 1 & & & \\ -0.09 & -0.08 & 1 & & \\ 0.04 & -0.05 & -0.54 & 1 & \\ 0.08 & 0.08 & -0.04 & -0.54 & 1 \end{pmatrix}.$$

In this work we do not make any flavour hypothesis and use the results of [58]. By adopting instead the results from the global fit in [81], which assumes the more constraining $U(3)^5$ -symmetry at high scale, the NP effect on the SABS cross section can be reduced approximately by a factor of four, which is however not enough for the NP contamination to be below the precision goal at the future e^+e^- machines.

Appendix B: Fit methodology

The asymmetries considered in this work are built from cross sections $\sigma_{a,b}$, where $\{a,b\} = \{F,B\}, \{L,R\}, \{\uparrow,\downarrow\}$ and defined as $A_{ab} = (\sigma_a - \sigma_b)/(\sigma_a + \sigma_b)$. In the hypothesis of independence from the luminosity, those asymmetries can be defined from the observed number of events as

$$A_{ab} = \frac{N_a - N_b}{N_a + N_b},$$

that can be estimated as $N_{a,b} = L \sigma_{a,b}$, with $L = \int \mathcal{L} dt$ the time integrated luminosity. The absolute statistical error on the number of events is given by $\Delta_{a,b} = \sqrt{N_{a,b}}$. Therefore, we propagate the error on the asymmetry assuming statistically independent measurements

$$\Delta A_{ab} = \sqrt{\sum_{k=a,b} \left(\frac{\partial A_{ab}}{\partial N_k} \right)^2 \Delta_k^2} = 2 \sqrt{\frac{N_a N_b}{(N_a + N_b)^3}}.$$

The theoretical prediction for A_{ab} in the SMEFT can be written as

$$A_{ab}^{\text{th}} = A_{ab}^{\text{SM}} \left\{ 1 + \frac{(\sigma_a - \sigma_b)^{(6)}}{(\sigma_a - \sigma_B)_{\text{SM}}} - \frac{(\sigma_a + \sigma_b)^{(6)}}{(\sigma_a + \sigma_b)_{\text{SM}}} \right\},$$

where $\sigma_{a,b}^{(6)} = \sum_i C_i / \Lambda_{\text{NP}}^2 \sigma_{a,b}^{(6),i}$ as in Eq. (10).

For the polarisation asymmetries considered in Section III B, the dependence on the WCs of the prediction in the SMEFT can be exploited to fit the values of C_i .

We consider $n = 78$ experimental bins in $\cos\theta$ of width $\Delta \cos\theta = 0.02$ and define $\mathbf{A}_\alpha \equiv \left(A_{ab}^0 - A_{ab}^{\text{th}}(\vec{C}) \right)_\alpha$, with $\alpha = 1, \dots, n$, as the difference between the experimental value and the theoretical prediction for the asymmetry in the α -th bin and the matrix W is the experimental correlation matrix. We are assuming the experimental values A_{ab}^0 to be uncorrelated and centered around the SM prediction A_{ab}^{SM} , with the statistical error described above. Therefore, in each bin α , the projected data is distributed as a Gaussian $A_{\text{pol},\alpha}^0 \sim g(A_{\text{pol}}^{\text{SM}}, \Delta A_{\text{pol}}^0)_\alpha$. We build a multivariate Gaussian likelihood [72] as follows

$$L(\vec{C}) = \mathcal{N} \exp \left\{ -\frac{1}{2} \mathbf{A}^T(\vec{C}) W^{-1} \mathbf{A}(\vec{C}) \right\},$$

where \mathcal{N} is a normalisation factor. Hence, the negative logarithm of the likelihood function $\chi^2(\vec{C}) = -2 \log L(\vec{C})$ is distributed as a chi-squared with the number of d.o.f. given by $\nu = \dim(\vec{C})$. Under these hypotheses, the χ^2 can be rewritten as

$$\chi^2(\vec{C}) = \frac{1}{\Lambda_{\text{NP}}^4} \sum_{i,j} \sum_{\alpha,\beta} C_i \kappa_{i,\alpha}^{(6)} W_{\alpha\beta}^{-1} \kappa_{j,\beta}^{(6)} C_j,$$

where $\kappa_{i,\alpha}^{(6)} = \partial A_{\text{pol},\alpha}^{\text{th}} / \partial C_i$ is the derivative of the SMEFT theoretical prediction. The matrix $V_{ij}^{-1} = \sum_{\alpha,\beta} \kappa_{i,\alpha}^{(6)} W_{\alpha\beta}^{-1} \kappa_{j,\beta}^{(6)}$ is the inverse covariance matrix between WCs. The amplitude $\Delta(C_i)$ of the 68% confidence interval on C_i is given by $\sqrt{V_{ii}}$. This is equivalent to the projection on the C_i -axis of the region in the space of WCs corresponding to $\chi^2(\vec{C}) \leq 1$.

-
- [1] S. Actis *et al.* (Working Group on Radiative Corrections, Monte Carlo Generators for Low Energies), Quest for precision in hadronic cross sections at low energy: Monte Carlo tools vs. experimental data, *Eur. Phys. J. C* **66**, 585 (2010), arXiv:0912.0749 [hep-ph].
- [2] S. Schael *et al.* (ALEPH, DELPHI, L3, OPAL, SLD, LEP Electroweak Working Group, SLD Electroweak Group, SLD Heavy Flavour Group), Precision electroweak measurements on the Z resonance, *Phys. Rept.* **427**, 257 (2006), arXiv:hep-ex/0509008.
- [3] G. Voutsinas, E. Perez, M. Dam, and P. Janot, Beam-beam effects on the luminosity measurement at LEP and the number of light neutrino species, *Phys. Lett. B* **800**, 135068 (2020), arXiv:1908.01704 [hep-ex].
- [4] P. Janot and S. Jadach, Improved Bhabha cross section at LEP and the number of light neutrino species, *Phys. Lett. B* **803**, 135319 (2020), arXiv:1912.02067 [hep-ph].
- [5] J. de Blas *et al.*, Focus topics for the ECFA study on Higgs / Top / EW factories, arXiv:2401.07564 [hep-ph] (2024).
- [6] G. Abbiendi *et al.* (OPAL), Precision luminosity for $Z0$ line shape measurements with a silicon tungsten calorimeter, *Eur. Phys. J. C* **14**, 373 (2000), arXiv:hep-ex/9910066.
- [7] S. Jadach, W. Placzek, M. Skrzypek, B. F. L. Ward, and S. A. Yost, The path to 0.01% theoretical luminosity precision for the FCC-ee, *Phys. Lett. B* **790**, 314 (2019), arXiv:1812.01004 [hep-ph].
- [8] S. Abreu *et al.*, Theory for the FCC-ee: Report on the 11th FCC-ee Workshop Theory and Experiments, arXiv:1905.05078 [hep-ph] (2019).
- [9] B. F. L. Ward, S. Jadach, W. Placzek, M. Skrzypek, and S. A. Yost, Path to the 0.01% Theoretical Luminosity Precision Requirement for the FCC-ee (and ILC), in *International Workshop on Future Linear Colliders* (2019) arXiv:1902.05912 [hep-ph].
- [10] B. F. L. Ward, S. Jadach, W. Placzek, M. Skrzypek, and S. A. Yost, Overview of the Path to 0.01% Theoretical Luminosity Precision for the FCC-ee and Its Possible Synergistic Effects for Other FCC Precision Theory Requirements, *PoS ICHEP2020*, 704 (2021), arXiv:2012.11437 [hep-ph].
- [11] S. Jadach, W. Placzek, M. Skrzypek, and B. F. L. Ward, Study of theoretical luminosity precision for electron colliders at higher energies, *Eur. Phys. J. C* **81**, 1047 (2021).
- [12] M. Skrzypek, W. Placzek, B. F. L. Ward, and S. Y. Yost, How Well Could We Calculate Luminosity at FCCee?, *Acta Phys. Polon. Supp.* **17**, 2 (2024).

- [13] B. F. L. Ward, S. Jadach, W. Placzek, M. Skrzypek, and S. A. Yost, Outlook for the Theoretical Precision of the Luminosity at Future Lepton Colliders, arXiv:2410.09095 [hep-ph] (2024).
- [14] J. A. Maestre, Precision studies of quantum electrodynamics at future e^+e^- colliders, arXiv:2206.07564 [hep-ph] (2022).
- [15] C. M. Carloni Calame, M. Chiesa, G. Montagna, O. Nicrosini, and F. Piccinini, Electroweak corrections to $e^+e^- \rightarrow \gamma\gamma$ as a luminosity process at FCC-ee, Phys. Lett. B **798**, 134976 (2019), arXiv:1906.08056 [hep-ph].
- [16] M. Dam, Challenges for FCC-ee luminosity monitor design, Eur. Phys. J. Plus **137**, 81 (2022), arXiv:2107.12837 [physics.ins-det].
- [17] A. Abada *et al.* (FCC), FCC Physics Opportunities: Future Circular Collider Conceptual Design Report Volume 1, Eur. Phys. J. C **79**, 474 (2019).
- [18] A. Abada *et al.* (FCC), FCC-ee: The Lepton Collider: Future Circular Collider Conceptual Design Report Volume 2, Eur. Phys. J. ST **228**, 261 (2019).
- [19] CEPC Conceptual Design Report: Volume 1 - Accelerator, arXiv:1809.00285 [physics.acc-ph] (2018).
- [20] M. Dong *et al.* (CEPC Study Group), CEPC Conceptual Design Report: Volume 2 - Physics & Detector, arXiv:1811.10545 [hep-ex] (2018).
- [21] The International Linear Collider Technical Design Report - Volume 1: Executive Summary, arXiv:1306.6327 [physics.acc-ph] (2013).
- [22] The International Linear Collider Technical Design Report - Volume 2: Physics, arXiv:1306.6352 [hep-ph] (2013).
- [23] The International Linear Collider Technical Design Report - Volume 3.I: Accelerator & in the Technical Design Phase, arXiv:1306.6353 [physics.acc-ph] (2013).
- [24] The International Linear Collider Technical Design Report - Volume 3.II: Accelerator Baseline Design, arXiv:1306.6328 [physics.acc-ph] (2013).
- [25] H. Abramowicz *et al.*, The International Linear Collider Technical Design Report - Volume 4: Detectors, arXiv:1306.6329 [physics.ins-det] (2013).
- [26] Physics and Detectors at CLIC: CLIC Conceptual Design Report, arXiv:1202.5940 [physics.ins-det] (2012).
- [27] M. J. Boland *et al.* (CLIC, CLICdp), Updated baseline for a staged Compact Linear Collider, arXiv:1608.07537 [physics.acc-ph] (2016).
- [28] T. K. Charles *et al.* (CLICdp, CLIC), The Compact Linear Collider (CLIC) - 2018 Summary Report, arXiv:1812.06018 [physics.acc-ph] (2018).
- [29] T. Hahn, Generating Feynman diagrams and amplitudes with FeynArts 3, Comput. Phys. Commun. **140**, 418 (2001), arXiv:hep-ph/0012260.
- [30] R. Mertig, M. Bohm, and A. Denner, FEYN CALC: Computer algebraic calculation of Feynman amplitudes, Comput. Phys. Commun. **64**, 345 (1991).
- [31] V. Shtabovenko, R. Mertig, and F. Orellana, New Developments in FeynCalc 9.0, Comput. Phys. Commun. **207**, 432 (2016), arXiv:1601.01167 [hep-ph].
- [32] A. Dedes, W. Materkowska, M. Paraskevas, J. Rosiek, and K. Suxho, Feynman rules for the Standard Model Effective Field Theory in R_ξ -gauges, JHEP **06**, 143, arXiv:1704.03888 [hep-ph].
- [33] A. Dedes, M. Paraskevas, J. Rosiek, K. Suxho, and L. Trifyllis, SmeftFR – Feynman rules generator for the Standard Model Effective Field Theory, Comput. Phys. Commun. **247**, 106931 (2020), arXiv:1904.03204 [hep-ph].
- [34] A. Dedes, J. Rosiek, M. Ryczkowski, K. Suxho, and L. Trifyllis, SmeftFR v3 – Feynman rules generator for the Standard Model Effective Field Theory, Comput. Phys. Commun. **294**, 108943 (2024), arXiv:2302.01353 [hep-ph].
- [35] I. Brivio, Y. Jiang, and M. Trott, The SMEFTsim package, theory and tools, JHEP **12**, 070, arXiv:1709.06492 [hep-ph].
- [36] I. Brivio, SMEFTsim 3.0 — a practical guide, JHEP **04**, 073, arXiv:2012.11343 [hep-ph].
- [37] J. Alwall, R. Frederix, S. Frixione, V. Hirschi, F. Maltoni, O. Mattelaer, H. S. Shao, T. Stelzer, P. Torrielli, and M. Zaro, The automated computation of tree-level and next-to-leading order differential cross sections, and their matching to parton shower simulations, JHEP **07**, 079, arXiv:1405.0301 [hep-ph].
- [38] A. Alloul, N. D. Christensen, C. Degrande, C. Duhr, and B. Fuks, FeynRules 2.0 - A complete toolbox for tree-level phenomenology, Comput. Phys. Commun. **185**, 2250 (2014), arXiv:1310.1921 [hep-ph].
- [39] C. M. Carloni Calame, C. Lunardini, G. Montagna, O. Nicrosini, and F. Piccinini, Large angle Bhabha scattering and luminosity at flavor factories, Nucl. Phys. B **584**, 459 (2000), arXiv:hep-ph/0003268.
- [40] C. M. Carloni Calame, An Improved parton shower algorithm in QED, Phys. Lett. B **520**, 16 (2001), arXiv:hep-ph/0103117.
- [41] G. Balossini, C. M. Carloni Calame, G. Montagna, O. Nicrosini, and F. Piccinini, Matching perturbative and parton shower corrections to Bhabha process at flavour factories, Nucl. Phys. B **758**, 227 (2006), arXiv:hep-ph/0607181.
- [42] G. Balossini, C. Bignamini, C. M. C. Calame, G. Montagna, O. Nicrosini, and F. Piccinini, Photon pair production at flavour factories with per mille accuracy, Phys. Lett. B **663**, 209 (2008), arXiv:0801.3360 [hep-ph].
- [43] E. Budassi, C. M. Carloni Calame, M. Ghilardi, A. Gurgone, G. Montagna, M. Moretti, O. Nicrosini, F. Piccinini, and F. P. Ucci, Pion pair production in e^+e^- annihilation at next-to-leading order matched to Parton Shower, arXiv:2409.03469 [hep-ph] (2024).
- [44] A. Masiero, P. Paradisi, and M. Passera, New physics at the MUonE experiment at CERN, Phys. Rev. D **102**, 075013 (2020), arXiv:2002.05418 [hep-ph].
- [45] Y. M. Andreev *et al.* (NA64), Constraints on New Physics in Electron $g - 2$ from a Search for Invisible Decays of a Scalar, Pseudoscalar, Vector, and Axial Vector, Phys. Rev. Lett. **126**, 211802 (2021), arXiv:2102.01885 [hep-ex].
- [46] F. Acanfora, R. Franceschini, A. Mastroddi, and D. Redigolo, Fusing photons into nothing, a new search for invisible ALPs and Dark Matter at Belle II, JHEP **11**, 156, arXiv:2307.06369 [hep-ph].
- [47] F. Nguyen, F. Piccinini, and A. D. Polosa, $e^+e^- \rightarrow e^+e^-\pi^0\pi^0$ at DAPHNE, Eur. Phys. J. C **47**, 65 (2006), arXiv:hep-ph/0602205.
- [48] D. Babusci *et al.* (KLOE-2), Measurement of η meson production in $\gamma\gamma$ interactions and $\Gamma(\eta \rightarrow \gamma\gamma)$ with the KLOE detector, JHEP **01**, 119, arXiv:1211.1845 [hep-ex].
- [49] E. Budassi, C. M. Carloni Calame, C. L. Del Pio, and F. Piccinini, Single π^0 production in μe scattering at MUonE, Phys. Lett. B **829**, 137138 (2022),

- arXiv:2203.01639 [hep-ph].
- [50] J. P. Lees *et al.* (BaBar), Search for Invisible Decays of a Dark Photon Produced in e^+e^- Collisions at BaBar, *Phys. Rev. Lett.* **119**, 131804 (2017), arXiv:1702.03327 [hep-ex].
- [51] S. J. Brodsky, T. Kinoshita, and H. Terazawa, Two Photon Mechanism of Particle Production by High-Energy Colliding Beams, *Phys. Rev. D* **4**, 1532 (1971).
- [52] B. Holdom, Two U(1)'s and Epsilon Charge Shifts, *Phys. Lett. B* **166**, 196 (1986).
- [53] C. Boehm and P. Fayet, Scalar dark matter candidates, *Nucl. Phys. B* **683**, 219 (2004), arXiv:hep-ph/0305261.
- [54] M. Pospelov, A. Ritz, and M. B. Voloshin, Secluded WIMP Dark Matter, *Phys. Lett. B* **662**, 53 (2008), arXiv:0711.4866 [hep-ph].
- [55] M. Bauer, P. Foldenauer, and J. Jaeckel, Hunting All the Hidden Photons, *JHEP* **07**, 094, arXiv:1803.05466 [hep-ph].
- [56] N. Nath, N. Okada, S. Okada, D. Raut, and Q. Shafi, Light Z' and Dirac fermion dark matter in the $B-L$ model, *Eur. Phys. J. C* **82**, 864 (2022), arXiv:2112.08960 [hep-ph].
- [57] I. Brivio and M. Trott, The Standard Model as an Effective Field Theory, *Phys. Rept.* **793**, 1 (2019), arXiv:1706.08945 [hep-ph].
- [58] A. Falkowski, M. González-Alonso, and K. Mimouni, Compilation of low-energy constraints on 4-fermion operators in the SMEFT, *JHEP* **08**, 123, arXiv:1706.03783 [hep-ph].
- [59] B. Grzadkowski, M. Iskrzynski, M. Misiak, and J. Rosiek, Dimension-Six Terms in the Standard Model Lagrangian, *JHEP* **10**, 085, arXiv:1008.4884 [hep-ph].
- [60] A. Biekötter, B. D. Pecjak, D. J. Scott, and T. Smith, Electroweak input schemes and universal corrections in SMEFT, *JHEP* **07**, 115, arXiv:2305.03763 [hep-ph].
- [61] S. Dawson and P. P. Giardino, Electroweak and QCD corrections to Z and W pole observables in the standard model EFT, *Phys. Rev. D* **101**, 013001 (2020), arXiv:1909.02000 [hep-ph].
- [62] S. Dawson and P. P. Giardino, New physics through Drell-Yan standard model EFT measurements at NLO, *Phys. Rev. D* **104**, 073004 (2021), arXiv:2105.05852 [hep-ph].
- [63] K. Asteriadis, S. Dawson, P. P. Giardino, and R. Szafron, Impact of Next-to-Leading-Order Weak Standard-Model-Effective-Field-Theory Corrections in $e^+e^- \rightarrow ZH$, *Phys. Rev. Lett.* **133**, 231801 (2024), arXiv:2406.03557 [hep-ph].
- [64] K. Asteriadis, S. Dawson, P. P. Giardino, and R. Szafron, The $e^+e^- \rightarrow ZH$ Process in the SMEFT Beyond Leading Order, arXiv:2409.11466 [hep-ph] (2024).
- [65] S. Dawson, M. Forsslund, and P. P. Giardino, NLO SMEFT Electroweak Corrections to Higgs Decays to 4 Leptons in the Narrow Width Approximation, arXiv:2411.08952 [hep-ph] (2024).
- [66] R. Bartocci, A. Biekötter, and T. Hurth, Renormalisation group evolution effects on global SMEFT analyses, arXiv:2412.09674 [hep-ph] (2024).
- [67] E. Celada, T. Giani, J. ter Hoeve, L. Mantani, J. Rojo, A. N. Rossia, M. O. A. Thomas, and E. Vryonidou, Mapping the SMEFT at high-energy colliders: from LEP and the (HL-)LHC to the FCC-ee, *JHEP* **09**, 091, arXiv:2404.12809 [hep-ph].
- [68] We have verified that, by taking $\alpha(0)$ instead of $\alpha(M_Z)$ as input, the results change by a factor $\alpha(M_Z)/\alpha(0)$, which is well within the 68% error $\Delta\delta_{\text{SMEFT}}$.
- [69] G. Montagna, O. Nicrosini, and F. Piccinini, Precision physics at LEP, *Riv. Nuovo Cim.* **21N9**, 1 (1998), arXiv:hep-ph/9802302.
- [70] Should the real data give values for the WCs not compatible with zero, this would be a clear indication of NP.
- [71] We checked, through BABAYAGA@NLO simulation with QED leading logarithmic corrections switched on, that the shape of the plot of Fig. 1 is preserved, the largest shift affecting the second local minimum, which moves to about 103 GeV.
- [72] L. Berthier and M. Trott, Consistent constraints on the Standard Model Effective Field Theory, *JHEP* **02**, 069, arXiv:1508.05060 [hep-ph].
- [73] K. Abe *et al.* (SLD), Precise measurement of the left-right cross-section asymmetry in Z boson production by e^+e^- collisions, *Phys. Rev. Lett.* **73**, 25 (1994), arXiv:hep-ex/9404001.
- [74] Since we are considering a large-angle observable, going to higher energies could spoil the validity of the EFT. A low/intermediate energy run would therefore be important for precision measurements.
- [75] K. Abe *et al.* (SLD), Direct measurement of leptonic coupling asymmetries with polarized Z s, *Phys. Rev. Lett.* **79**, 804 (1997), arXiv:hep-ex/9704012.
- [76] K. Abe *et al.* (SLD), An Improved direct measurement of leptonic coupling asymmetries with polarized Z bosons, *Phys. Rev. Lett.* **86**, 1162 (2001), arXiv:hep-ex/0010015.
- [77] A. Aryshev *et al.* (ILC International Development Team), The International Linear Collider: Report to Snowmass 2021, arXiv:2203.07622 [physics.acc-ph] (2022).
- [78] S. Funatsu, H. Hatanaka, Y. Hosotani, Y. Orikasa, and N. Yamatsu, Bhabha scattering in the gauge-Higgs unification, *Phys. Rev. D* **106**, 015010 (2022), arXiv:2203.16030 [hep-ph].
- [79] C. Miller and J. M. Roney, Comparison of left-right asymmetry calculations in the Bhabha process at an upgraded SuperKEKB, arXiv:2411.16592 [hep-ph] (2024).
- [80] D. de Florian *et al.* (LHC Higgs Cross Section Working Group), Handbook of LHC Higgs Cross Sections: 4. Deciphering the Nature of the Higgs Sector, arXiv:1610.07922 [hep-ph] (2016).
- [81] R. Bartocci, A. Biekötter, and T. Hurth, A global analysis of the SMEFT under the minimal MFV assumption, *JHEP* **05**, 074, arXiv:2311.04963 [hep-ph].